

Experiments with an Underground Lens Waveguide

By D. GLOGE

(Manuscript received December 21, 1966)

A laser beam was transmitted over a distance of 1/2 mile in an underground iron pipe using glass lenses 400 feet apart. The beam deflection and the temperature gradient in the air-filled pipe was measured simultaneously over periods of several weeks. It was found that gradients up to $0.02^{\circ}\text{C}/\text{cm}$, changing with the season, accounted for beam displacements up to 2 cm on the lenses. Since all these deviations are slow and no other severe disturbance was noticed, the conclusion is that the transmission of optical beams underground is possible without evacuation of the conduit. Suggestions for the construction of such a beam waveguide are made which could reduce the mentioned temperature influence by a factor of 100.

I. INTRODUCTION

If a beam of coherent light is to be transmitted along the surface of the earth it will be necessary to redirect and focus it at intervals by means of lenses or mirrors to follow the terrain.^{1,2} Furthermore, it must be shielded from atmospheric temperature fluctuations which result in variations of the index of refraction. A laboratory experiment which, in a 100-m metal pipe, folded a transmission path back upon itself gave the impression that the atmospheric effects could be overcome by choosing the proper beam enclosure.^{3,4} Other experimenters, using a 1-km long pipe above ground, considered evacuation as the most reasonable means to avoid temperature effects.⁵ In any case, the transmission path would most likely be installed underground where temperature variations are much smaller than in the open air.

To gain information about the transmission characteristics in this case a $\frac{1}{2}$ -mile underground iron pipe was used to build a lens waveguide with focusing lenses 400 feet apart. The temperature field and the beam displacement in the tube were measured simultaneously and compared with theoretical estimates. This gave valuable indications for the construction of underground lens waveguides.

11. GROUND TEMPERATURE

The temperature distribution in the ground depends very much on the type of soil, on the moisture content, and on the character of the surface. The common feature of any soil, however, is a high heat capacity c and comparatively low conductivity κ which leads to very slow heat diffusion processes. To give a representative picture, a half space with constant c and κ is considered. Then heat diffuses only along the vertical direction y and the temperature T can be found from the equation

$$\frac{\partial T}{\partial t} = \alpha \frac{\partial^2 T}{\partial y^2}, \quad (1)$$

where the ratio

$$\alpha = \frac{\kappa}{c} \quad (2)$$

is called the thermal diffusivity.

Since the temperature changes at the surface are mainly periodic it is convenient to consider the Fourier amplitudes T_ω of components with frequency ω . The solution of (1) in complex form is then

$$T(y, \omega) = T_\omega \exp(i\omega t - y\sqrt{i\omega/\alpha}). \quad (3)$$

The temperature is retarded and attenuated with increasing depth and increasing frequency.

To find the diffusivity α involved in this experiment, thermocouples were installed 0, 1, and 3 feet below the surface. A recording over 2 weeks is shown in Figs. 1(a) and (b). A comparison of the temperatures at the surface and 1 foot below show that a 1-foot layer of soil reduces the amplitude of the diurnal temperature cycle by a factor of 10 and introduces a phase lag of 10 hours. This corresponds to a diffusivity of $\alpha = 5.5 \cdot 10^{-3} \text{ cm}^2/\text{s}$.

Data gathered at different locations in the United States yield an average diffusivity of $5.4 \cdot 10^{-3} \text{ cm}^2/\text{s}$.⁴ Handbook data for clay soil are shown in Table I. According to these data the diurnal temperature cycle at a 3-foot depth is reduced by three orders of magnitude and therefore not noticeable in Fig. 1(b).

The recording of Fig. 1(c) shows the temperature gradient in the iron pipe 5 feet below the surface, which was used for the transmission experiment. This gradient was measured by a digital quartz thermometer whose sensors were installed at the top and the bottom of the tube. These sensors are connected with the equipment by 100 feet of cable so that the measurements could be taken far inside the tube and remote

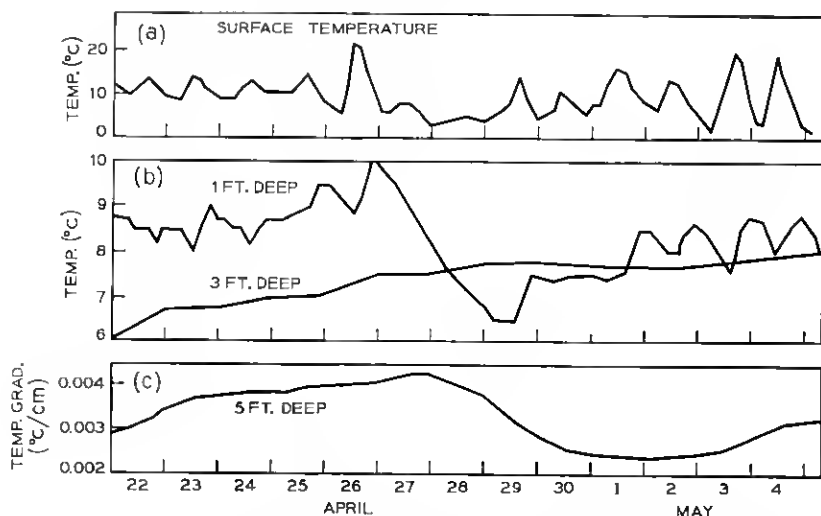


Fig. 1—Temperature recordings at Bell Telephone Laboratories, Holmdel, N. J. from April 22 to May 4, 1966. (a) Temperature at the surface. (b) Temperature at a depth of 1 and 3 ft. (c) Thermal gradient in an iron pipe with a wall thickness of $\frac{1}{4}$ " and an i.d. of 3.5" at a depth of 5 ft.

from any disturbance. No diurnal temperature changes were noticeable.

From (3) one finds the temperature gradient in the soil to be

$$\partial_z = \frac{\partial T}{\partial y} = -T_\omega \sqrt{i \frac{\omega}{\alpha}} \exp(i\omega t - y \sqrt{i\omega/\alpha}). \quad (4)$$

Gradients of very low and very high frequency disappear at a large enough depth. If the Fourier spectrum of the temperature on the surface is assumed to be flat then Fig. 2 gives the amplitude spectrum of the gradient at various depths.

TABLE I

		Still air	Clay soil	Steel	Alumi- num	Fiber- glass
Conductivity κ	$\frac{\text{cal}}{\text{cm s}^\circ\text{C}}$	$5.5 \cdot 10^{-5}$	$2.8 \cdot 10^{-3}$	0.11	0.55	10^{-4}
Heat capacity c	$\frac{\text{cal}}{\text{cm}^3 \cdot ^\circ\text{C}}$	$3 \cdot 10^{-4}$	0.5	1	0.65	—
Diffusivity α	$\frac{\text{cm}^2}{\text{s}}$	0.18	$5.4 \cdot 10^{-3}$	0.1	0.85	—

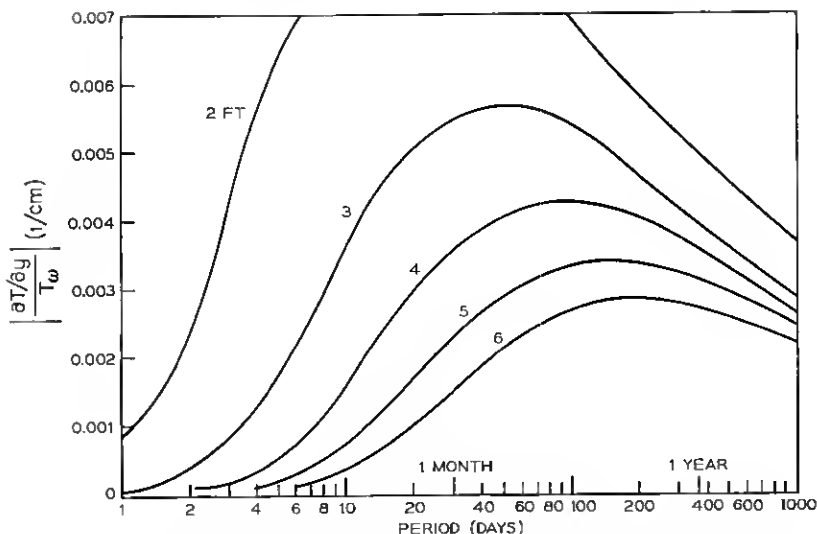


Fig. 2—Amplitude spectrum of the thermal gradient at various depths related to the amplitude at the surface of the ground.

Actually, the temperature spectrum at the surface is not constant but has peaks with periods of 1 day and 1 year. About 1 year is also the period which causes maximum response of the temperature gradient at a depth of 5 feet.

The mean temperature behavior valid for the area of New Jersey, as shown in Fig. 3, is based on data gathered in Ref. 6. The corresponding temperature cycle at a depth of 5 feet was calculated from (2). The dots show measured values. The presence of an air-filled iron pipe distorts the temperature field considerably. As is shown in the appendix, a function describing this field can be derived from an equivalent problem in the theory of electrostatic fields. Assuming that ϑ_s , the gradient in the absence of a tube, is approximately constant over an area comparable to the tube crosssection, the field inside the tube is found to be homogeneous having a thermal gradient ϑ_i that is given by (18).

For the tube used the inner radius $r_1 = 1.75$ inches, the outer radius $r_2 = 2$ inches and κ_0 , κ_1 , and κ_2 are the thermal conductivities of air, iron, and soil, respectively (see Fig. 4). With the numbers given in Table I, one finds that the internal gradient ϑ_i is reduced by a factor of 0.4 in comparison with ϑ_s . Therefore,

$$\vartheta_i = 0.4 \sqrt{i \frac{\omega}{\alpha}} \exp(i\omega t - y \sqrt{i\omega/\alpha}). \quad (5)$$

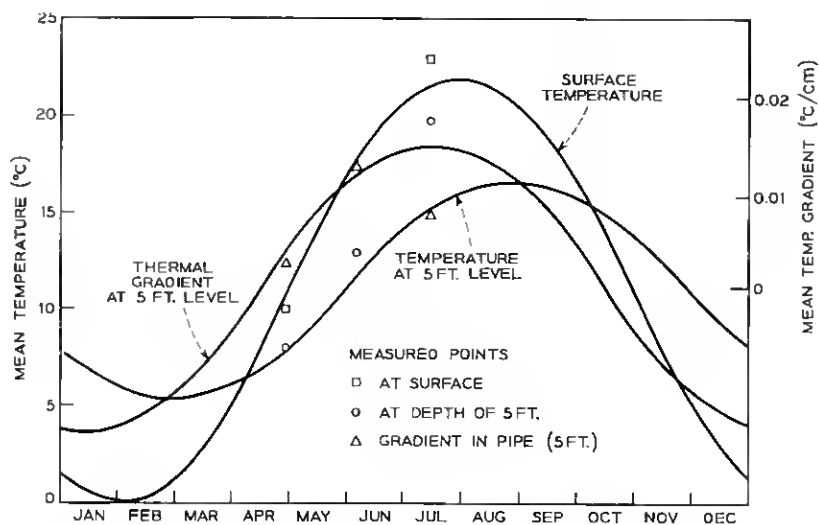


Fig. 3—Mean annual change of the temperature at the surface and at a depth of 5 ft and the corresponding thermal gradient in an iron pipe at a depth of 5 ft as expected from data given in Ref. 7. The dots show values measured at Bell Telephone Laboratories, Holmdel, N. J. in 1966.

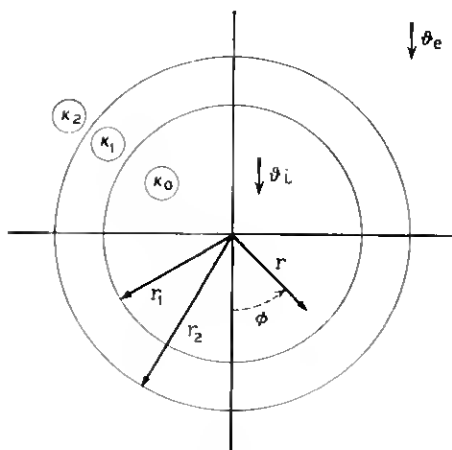


Fig. 4—Sketch of the pipe arrangement used to derive the internal temperature field.

As long as the thermal gradient has no horizontal component and its value is below a certain threshold, convection cannot develop in a cylindrical container.⁷ For the air-filled tube with the given dimensions, this threshold is $0.02^{\circ}\text{C}/\text{cm}$.

III. THE LENS WAVEGUIDE

The experimental setup as shown in Fig. 5(a) makes use of a straight iron pipe of $\frac{1}{2}$ -mile length with an inner diameter of 3.5 inches at a mean depth of 5 feet. Roughly every 140 m there is access to the pipe through manholes. Here biconvex thin lenses with a focal length of 70 m are installed.

The fundamental mode of this confocal lens waveguide is a beam with Gaussian field distribution. Operating at the laser wavelength of 0.63μ , the $1/e$ width of the field at the lenses is $2\sqrt{140 \text{ m } 0.63 \mu/\pi} = 10.4 \text{ mm}$. The lenses are supported by the pipe itself and mounted close to the wall of the manhole where the pipe comes out of the ground. No vibrations were noticed. The conduit is airtight over the whole transmission length.

The lenses have a diameter of 60 mm and can be adjusted for about

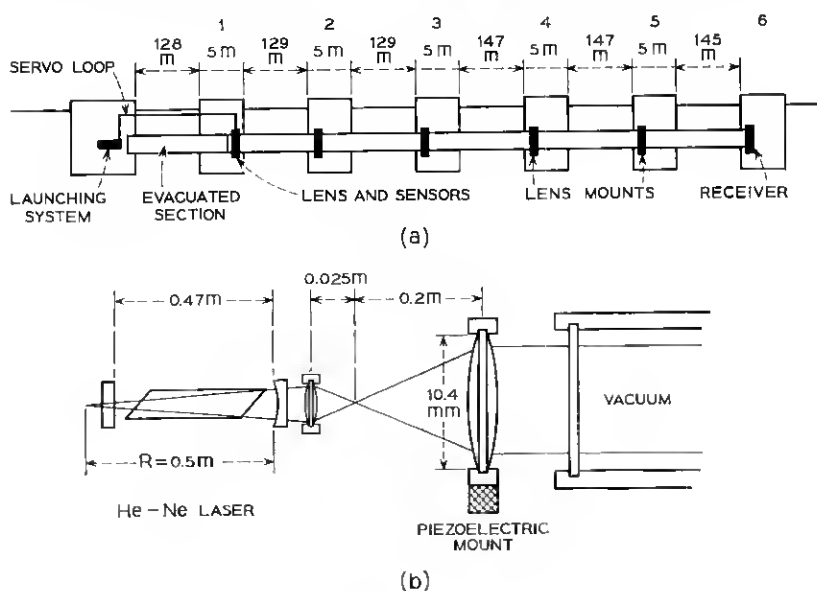


Fig. 5—Sketch of the experimental setup: (a) The transmission path. (b) The launching system.

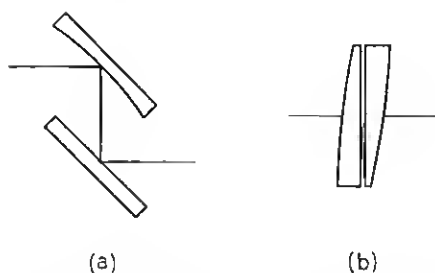


Fig. 6—Possible redirecting devices in a lens waveguide. (a) Mirror arrangement as proposed by Kompfner.¹ (b) Rotatable split lens which contains a variable prism.

± 15 mm from the outside of the pipe. This is sufficient to guide the beam in the conduit which is straight over the total length of $\frac{1}{2}$ mile. Of course, aligned sections cannot be expected in an actual field installation. Redirecting devices must therefore be provided where the described model has only focusing lenses.

In order to gain a feeling for the usefulness of the described model, some thought will be devoted to the features of redirecting devices. Fig. 6 shows two examples. In Fig. 6(a) a plain and a curved mirror are mounted opposite to each other.¹ Fig. 6(b) shows two eccentric parts of semiconvex lenses which can be rotated independently. The space between the adjacent surfaces is filled with an oil film which has the same refractive index as the lenses. The complete device acts therefore as a lens plus a variable prism.

The device in Fig. 6(a), as well as the one in Fig. 6(b), uses two (but not more than two) reflecting or refracting surfaces both to direct and to focus the beam. Those surfaces determine essentially the transmission loss in an optical waveguide.^{3,4,5} Therefore, redirection of the beam may be achieved without a large increase of the transmission loss, no matter if reflection or refraction is used. The experiment described here was started with refracting devices since they are easier to mount and to adjust, but an experiment with reflecting devices is planned as well.

The lenses used in the experiment have a surface quality of $\lambda/10$ and are furnished with an antireflection coating which guarantees less than 0.2 percent reflection at 0.63μ wavelength. The bandwidth is about 500 \AA . The absorption loss of the lens material is in the order of 0.02 percent for a lens thickness of 5 mm. Assuming a total absorption loss of 0.1 percent in the glass and the layers of the two coatings, an

overall loss of 0.5 percent must be expected per lens. (This varies by about ± 0.05 percent since the reflections from both surfaces interfere with each other and the total reflection therefore depends on the lens thickness.)

A loss of the same order for mirrors was reported in Ref. 3. No significant variations of the loss are therefore to be expected in this case. For the mean lens spacing of 140 m a waveguide loss of 0.15 dB/km would occur. This, of course, holds only for perfectly clean surfaces. A considerable increase of the loss must be expected if dust accumulates on the lenses. No loss measurements have been performed up to the present time.

The Gaussian field distribution is generated in the almost concentric resonator of a He-Ne laser and magnified by a factor of 8 in the lens arrangement shown in Fig. 5(b). These lenses are polished to a quality of $\lambda/10$ but are not corrected for aberrations.

The launching system consisting of laser and magnifier as shown in Fig. 5(h) is mounted on a solid concrete table resting on a 1-foot thick concrete floor. Although the air temperature around the launching system is kept constant within 2°C the temperature changes in the environment are large enough to cause deviations of the proper launching angle of $1.5 \cdot 10^{-5}$ rad or 2 mm at the first lens. To eliminate this effect a servo-loop was built which holds the beam center at the first lens within an area of $30 \times 30 \mu$. Of course no temperature effect can now be measured in the first pipe section, but by evacuating this section it is possible to attain a deviation angle of the forthcoming beam of no more than $30 \mu/128 \text{ m} = 2.3 \cdot 10^{-7}$ rad.

To measure the displacement of the beam the circuit in Fig. 7(a) was used. If the shown CdS-cells have the resistances R_1 and R_2 the output voltage is

$$V = \frac{V_o}{2} \frac{R_1 - R_2}{R_1 + R_2}. \quad (6)$$

Since these resistances, in the region used, are inversely proportional to the illuminating intensity I , (6) can also be written in the form

$$V = \frac{V_o}{2} \frac{I_2 - I_1}{I_2 + I_1}. \quad (7)$$

This shows that the output voltage does not depend on the absolute laser intensity but only on the ratio of the intensities absorbed by the resistors, which is a function of the displacement d and the beam width. A typical sensitivity curve of the device is shown in Fig. 7(b). The

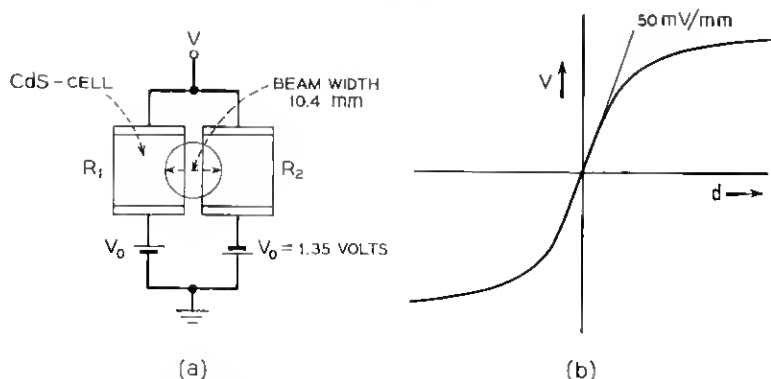


Fig. 7—Device to measure the beam displacement with photoresistors. (a) The circuit. (b) The sensitivity curve.

same circuits were used to produce the horizontal and the vertical feedback signals and to measure the beam movement at the end of the transmission path.

IV. BEAM DISPLACEMENT

Assume only small deviation of the beam from the ideal propagation axis z . Then the displacement d in a transverse direction y can be calculated from the equation

$$\frac{\partial^2 d}{\partial z^2} = \frac{1}{n} \frac{\partial n}{\partial y}. \quad (8)$$

Here n is the refractive index which for air at atmospheric pressure has the temperature dependence

$$n = 1 + \Delta n \frac{T_o}{T} \quad (9)$$

with $\Delta n = 3 \cdot 10^{-4}$. This yields

$$\frac{\partial^2 d}{\partial z^2} = -\frac{\Delta n}{n} \frac{1}{T_o} \frac{\partial T}{\partial y}. \quad (10)$$

If $\partial T / \partial y$ is assumed constant over a transmission length L a simple integration of (10) gives the displacement

$$d = -\frac{\Delta n}{2n} \frac{L^2}{T_o} \frac{\partial T}{\partial y} \quad (11)$$

at the end of the path L , provided the beam is injected on axis at the beginning. To measure this effect the stabilized beam coming out of the evacuated pipe section was sent through the next section and its displacement recorded in the second manhole. At the same time the temperature gradient was measured in another pipe section. Inserting these values into (11) the expected beam displacement was calculated. The thermal gradient and the measured and calculated displacement are shown in Fig. 8. There are short-term movements superimposed on the main slope which are caused by diurnal temperature changes in the manholes. Here the pipe warms up over the day and cools down at night. This introduces convection currents along the pipe which cause a transverse temperature gradient and a deflection of the beam.⁷

Recordings of the beam position over the full transmission length again showed diurnal deviations (up to 4 mm) introduced by the temperature change in the manholes.

So far only changes of the temperature gradient have been considered but nothing has been said about the absolute gradient. Fig. 3 shows that a maximum gradient of $\pm 0.02^\circ\text{C}/\text{cm}$ must be expected. In this case, if the beam enters the waveguide on axis, the displacement on the second lens according to (11) is 2 cm. The third lens is passed at

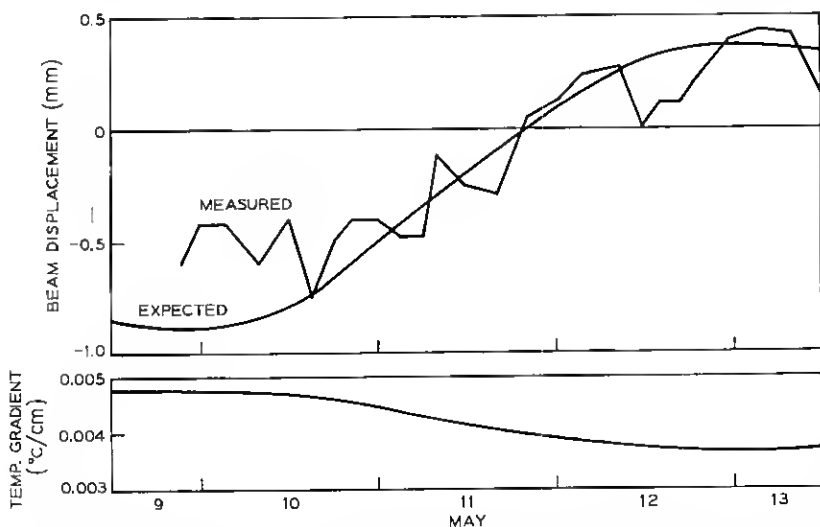


Fig. 8—Measured and expected beam displacement as calculated from the thermal gradient shown below for a laser beam transmitted over 128 m through an iron pipe at a depth of 5 feet in the ground.

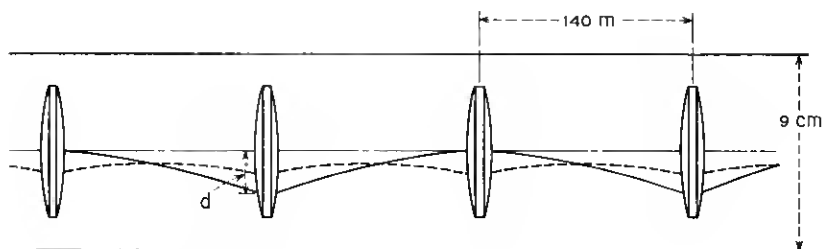


Fig. 9—Beam path in the experimental lens waveguide at the time of maximum temperature gradient.

the center, but at the fourth lens again 2-cm displacement occurs. The beam undulates about the dotted line shown in Fig. 9. A proper launching of the beam would avoid the undulations and the beam would follow the dotted line. This behavior was indeed found quantitatively during measurements in June when a high temperature gradient occurred.

Since the beam center has to pass a lens at least 1 cm from the lens edge to avoid noticeable diffraction, the described lens waveguide can just handle the occurring temperature effect. Of course, this waveguide runs below a uniform grass surface and the temperature gradient is fairly constant everywhere. An actual transmission path, however, will be subject to changes of the temperature gradient from section to section and that will cause undulations of the beam which increase with the transmission length. For this reason a thermal gradient as great as that measured would be a serious drawback for the waveguide and a considerable reduction of the temperature influence in the conduit seems necessary.

This can be accomplished by employing a pipe material of higher conductivity. The reduction factor ∂_i/∂_e calculated from (18) is shown in Fig. 10 for iron and aluminum tubes with various diameter ratios. Using an aluminum pipe instead of the present iron pipe would reduce the inside thermal gradient by a factor of 5.

The shielding effect can be improved even more by using several coaxial layers of strongly alternating conductivity. As a practical example for a triple-layer pipe, the combination aluminum-concrete-aluminum was calculated using a concrete volume three times larger than the aluminum volume. The thickness of the layers is chosen in such a way that the shielding effect is largest. As Fig. 10 shows, such a pipe can be more effective than a solid aluminum pipe if the layers

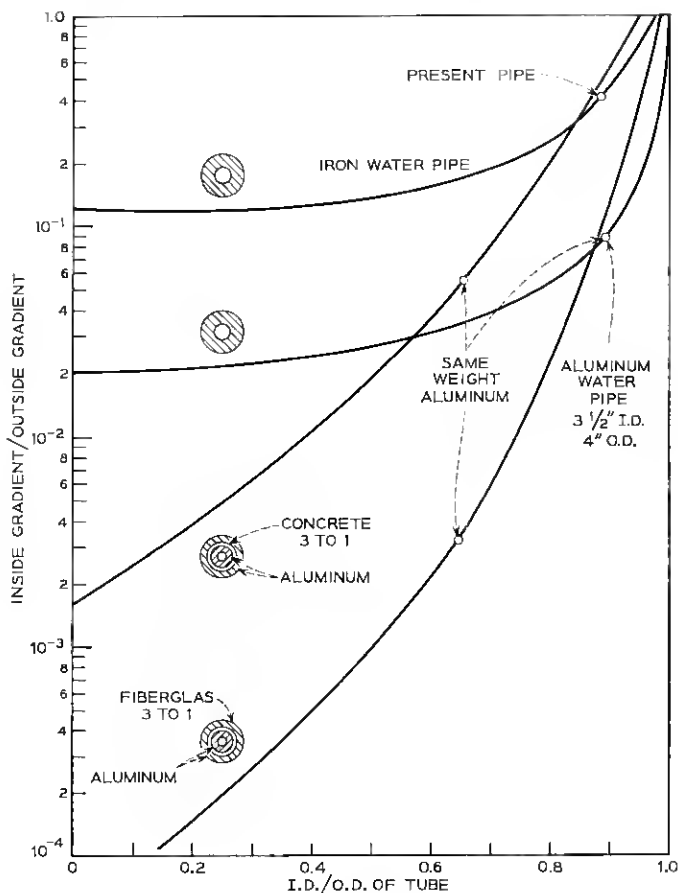


Fig. 10—The reduction factor versus the ratio of inside to outside diameter for a solid iron pipe, a solid aluminum pipe and aluminum pipes stacked with concrete and fiberglass using a volume ratio 1:3.

are very thick. For the same amount of aluminum as in the solid tube, however, it is only a factor of $\frac{2}{3}$ better.

Using fiberglass instead of concrete improves the shielding effect considerably. A pipe with the same aluminum weight as before yields a reduction factor of $3 \cdot 10^{-3}$. Compared with the iron water pipe now in use, the shielding effect of the latter arrangement is two orders of magnitude better, and the maximum expected gradient in such a pipe would therefore be $2 \cdot 10^{-4}^{\circ}\text{C}/\text{cm}$.

V. CONCLUSIONS

The results of the described experiment show that the main disturbance of a coherent light beam transmitted in an air-filled underground conduit is a slowly varying displacement of the beam center. This displacement can be coordinated with thermal gradients in the atmosphere of the pipe and predicted theoretically. No other time dependent sources of disturbance were noticed in the experiment. The mounting, as well as the adjustment of the lenses, was not critical.

To reduce the beam displacement to a tolerable amount some simple provisions must be made: (i) the conduit should be imbedded in the soil everywhere and exposure to temperature changes should be minimized; (ii) the conduit should be airtight to avoid longitudinal air currents; (iii) a tube of high thermal conductivity or a multilayer tube with a good shielding effect should be chosen. With the proper design no larger gradients than $0.001^{\circ}\text{C}/\text{cm}$ would occur in the pipe. If, for example, the gradient is not constant over the transmission path but varies with a rms value of $0.001^{\circ}\text{C}/\text{cm}$ then, if the lens spacing is 140 m and the beam enters on axis, beam undulations occur with a mean amplitude of 0.5 mm at the beginning of the waveguide, increasing to 5 mm after 100 lens sections. There the beam could be realigned by an electronic servo system.⁸

Drift and vibrations of the ground were not investigated until now, but these might very well cause larger displacements than the ones just mentioned. This would necessitate beam aligning servo systems at even shorter intervals.

VI. ACKNOWLEDGMENTS

The writer wishes to thank E. A. J. Marcatili and O. E. DeLange for many fruitful discussions and constructive suggestions. The assistance of H. Earl in alignment and operation is gratefully acknowledged.

APPENDIX

To find the temperature field in an around several coaxial cylinders of different material as shown in Fig. 4, the equivalent problem in the theory of electrostatic fields is considered. It is known that a circular dielectric rod with its axis perpendicular to a homogeneous electric field develops a homogeneous internal field determined by its polarization and an external field that consists of the superposition of the original field plus a field generated by the polarization of the rod.

In polar coordinates, a homogeneous temperature field with gradient ϑ_0 has the form $\vartheta_0 r \cos \varphi$ (see Fig. 4). If now a circular rod is brought into the field, an additional term of the form $(\theta/r^2) \cos \varphi$ arises originated by the "polarization" θ of the rod. In a more complicated configuration of several coaxial cylinders, the field in the various materials can still be described by terms of the above type.

Labeling the n layers starting with $\nu = 0$ for the center rod, one has for the field T_ν in the ν th layer

$$T_\nu = \vartheta_\nu r \cos \varphi + \frac{\theta_\nu}{r^2} \cos \varphi \quad (12)$$

for

$$\nu = 0, 1 \cdots n.$$

T_n is the field in the surrounding and $\vartheta_n \equiv \vartheta_0$, the original thermal gradient. $\theta_0 \equiv 0$ since the field in the center bore is homogeneous. This leaves $2n$ constants ϑ_ν and θ_ν . They can be found by matching the fields at the boundaries which yields $2n$ linear algebraic equations of the form

$$\vartheta_{\nu-1} - \frac{\theta_{\nu-1}}{r_\nu^2} = \vartheta_\nu - \frac{\theta_\nu}{r_\nu^2} \quad (13)$$

and

$$\kappa_{\nu-1} \left(\vartheta_{\nu-1} + \frac{\theta_{\nu-1}}{r_\nu^2} \right) = \kappa_\nu \left(\vartheta_\nu + \frac{\theta_\nu}{r_\nu^2} \right). \quad (14)$$

To calculate the internal gradient $\vartheta_i \equiv \vartheta_0$ it is convenient to define the ratios

$$p_\nu^+ = \frac{\kappa_{\nu-1} + \kappa_\nu}{2\kappa_\nu} \quad (15)$$

$$p_\nu^- = \frac{\kappa_{\nu-1} - \kappa_\nu}{2\kappa_\nu} \quad (16)$$

and a determinant

$$D_n = \begin{vmatrix} p_0^+ & \frac{r_1}{r_2} p_1^- & \cdots & -(-1)^n \frac{r_1}{r_n} p_n^- \\ -\frac{r_1}{r_2} p_0^- & p_1^+ & & -(-1)^{n-1} \frac{r_2}{r_n} p_n^- \\ \vdots & & & \\ (-1)^n \frac{r_1}{r_n} p_0^- & (-1)^{n-1} \frac{r_2}{r_n} p_1^- & & p_n^+ \end{vmatrix}. \quad (17)$$

Then

$$\frac{\vartheta_0}{\vartheta_e} = \frac{1}{D_n}.$$

This is the ratio by which the gradient inside a multilayer tube is reduced in comparison with the gradient in the homogeneous soil (in absence of that pipe). For a solid tube as shown in Fig. 4, $n = 2$ and one finds

$$\frac{\vartheta_0}{\vartheta_e} = \frac{1}{\frac{\kappa_0 + \kappa_1}{2\kappa_1} \frac{\kappa_1 + \kappa_2}{2\kappa_2} + \left(\frac{r_1}{r_2}\right)^2 \frac{\kappa_0 - \kappa_1}{2\kappa_1} \frac{\kappa_1 - \kappa_2}{2\kappa_2}}. \quad (18)$$

REFERENCES

1. Kompfner, R., unpublished work.
2. Goubau, G. and Christian, F. R., On the Guided Propagation of Electromagnetic Wave Beams, IRE Trans. *AP-9*, May, 1961, pp. 248-256.
3. DeLange, O. E., Losses Suffered by Coherent Light Redirected and Refocussed in an Enclosed Medium, B.S.T.J., *44*, February, 1965, pp. 283-302.
4. Seifert, G. and Gloge, D., Messungen an einer Optischen Pendelimpulsstrecke, Archiv El. Übertragung, *19*, November, 1965, pp. 633-635.
5. Goubau, G. and Christian, F. R., Loss Measurements with a Beam Waveguide for Long-Distance Transmission at Optical Frequencies, Proc. IEEE, *52*, December, 1964, p. 1739.
6. Grisby, C. M. and Shuhart, F. M., Earth Temperatures, unpublished work.
7. Gloge, D., Thermal Instabilities in Optical Waveguides, unpublished work.
8. Marcantili, E. A. J., Ray Propagation in Beam-Waveguides with Redirectors, B.S.T.J., *45*, January, 1966, pp. 105-115.

